Title

Endothelial Cell Response in Kawasaki Disease and Multisystem Inflammatory Syndrome in Children

Journal
International Journal of Molecular Sciences, 24(15)

ISSN
1661-6596

Authors
Kim, Jihoon
Shimizu, Chisato
He, Ming
et al.

Publication Date
2023

DOI
10.3390/ijms241512318

Peer reviewed

International Journal of *Molecular Sciences*

MDPI

Research Article

Endothelial Cell Response in Kawasaki Disease and Multisystem Inflammatory Syndrome in Children

Jihoon Kim [1,4*#], Chisato Shimizu [2#], Ming He [3], Hao Wang [2], Hal M. Hoffman [2,5], Adriana H. Tremoulet [2,5], John Y-J. Shyy [3], and Jane C. Burns [2,5]

[1] Department of Biomedical Informatics, [2] Department of Pediatrics, [3] Department of Medicine, University of California, San Diego
[4] Section of Biomedical Informatics and Data Science, Yale School of Medicine, New Haven, CT, [5] Rady Children's Hospital, San Diego, CA,

* Correspondence: c1shimizu@ucsd.edu
\# These authors contributed equally to this work

Abstract: Although Kawasaki disease (KD) and Multisystem inflammatory syndrome in children (MIS-C) share some clinical manifestations, their cardiovascular outcomes are different, and this may be reflected at the level of the endothelial cell (EC). We performed RNA-seq on cultured ECs incubated with pre-treatment sera from KD (n=5), MIS-C (n=7), and healthy controls (n=3). We conducted Weighted Gene Co-expression Network Analysis (WGCNA) using 935 transcripts differentially expressed between MIS-C and KD using relaxed filtering (un-adjusted p<0.05, >1.1 fold difference). We found seven gene modules in MIS-C annotated as increased TNFα/NFκB pathway, decreased EC homeostasis, anti-inflammation and immune response, translation, and glucocorticoid responsive genes and Endothelial-Mesenchymal Transition (EndoMT) suppression in MIS-C. To further understand the difference in the EC response between MIS-C and KD, a stringent filtering was applied to identify 41 differentially expressed genes (DEGs) between MIS-C and KD (adjusted p<0.05, >2 fold-difference). Again, in MIS-C, NFκB pathway genes including nine pro-survival genes were upregulated. Expression levels were higher in the genes influencing autophagy (*UBD*, *EBI3*, and *SQSTM1*). Other DEGs also supported the finding by WGCNA. Compared to KD, ECs in MIS-C had increased pro-survival transcripts, but reduced transcripts related to EndoMT and EC homeostasis. These differences in EC response may influence the different cardiovascular outcomes in these two diseases.

Keywords: Kawasaki disease; MIS-C; endothelial cell; WGCNA; network analysis; NFκB pathway; apoptosis; autophagy; EndoMT; RNAseq

1. Introduction

Kawasaki disease (KD) and Multisystem inflammatory syndrome in children (MIS-C) share some similar signs and symptoms [1]. Although patients with both diseases are highly inflamed, a disease classification algorithm using age, five clinical signs and 17 clinical laboratory values was able to distinguish MIS-C from KD and other febrile illnesses with >90% accuracy [2]. Increased inflammatory markers were among the key features in the classification algorithm that differentiated MIS-C from KD. The standard treatment for KD patients is intravenous immune globulin (IVIG), and 80-85% of patients respond to this treatment with cessation of fever [3, 4]. In contrast, MIS-C patients are also treated with IVIG but frequently require additional anti-inflammatory therapy including steroids and blockade of tumor necrosis factor (TNF)α and interleukin (IL)-1 [5].

The cardiovascular involvement in KD and MIS-C differs with transmural coronary artery inflammation resulting in coronary artery aneurysms associated only with KD. MIS-C, in contrast, commonly presents with decreased left ventricular contractility that reverses with anti-inflammatory therapy with no long-term sequelae in most patients [6]. There are only a limited number of autopsy reports describing clear cases of MIS-C but there is no long-term clinical vascular pathology associated with MIS-C [7, 8]. Molecular studies have compared and contrasted KD and MIS-C at the transcriptional and proteomic levels in circulating blood [9]. Upregulation of inflammatory pathways in both KD and MIS-C have underscored the similarities between the two conditions. We sought to characterize KD and MIS-C at the level of the EC to determine if the EC response might better reflect the divergent clinical outcomes of the two diseases.

To interrogate the EC response in patients with KD, we previously developed an experimental system using cultured endothelial cells (ECs) incubated with sera from pre-treatment KD patients [10]. Using that system, we demonstrated that ECs incubated with KD sera expressed a transcriptional profile associated with endothelial-mesenchymal transition (EndoMT) and altered EC homeostasis with reduced levels of nitric oxide synthase 3 (NOS3) [10]. To unravel the molecular mechanism of the divergent cardiovascular outcomes in KD and MIS-C, we studied transcriptional profiles of cultured ECs incubated with acute, pre-treatment sera from patients with either KD or MIS-C using RNA-seq.

2. Results

2.1. RNA-seq and differential expression analysis on cultured ECs incubated with sera from the patients with KD and MIS-C

To understand the EC response in KD and MIS-C, sera from five KD patients, seven MIS-C patients, and three healthy controls (HC) were incubated individually with cultured human umbilical vein ECs. RNA-seq was performed on cultured EC lysates (**Table 1**, **Figure 1**).

Table 1. Demographic and clinical characteristics of patients with KD and MIS-C whose sera were used in the EC experiment.

		MIS-C n=7	KD n=5	HC*4 n=3	P*5
Age, yrs*1		10.5 (8.8-12.2)	1.9 (1.6-3.8)	5.5 (4.2-7.1)	0.005
Male, n (%)		6 (86)	3 (60)	2 (67)	NS
Ethnicity, n (%)	Asian	0	1 (20)	0	NS
	AA	2 (29)	0	0	
	White	0	1 (20)	2 (67)	
	Hispanic	4 (57)	2 (40)	1 (33)	
	> 2 races	1 (14)	1 (20)	0	
Illness day of serum collection*2		3 (3-4.5)	5 (4-5)	418 (416-704)	NS
Coronary artery Zmax*3		2.1 (1.6-2.7)	3.2 (1.7-3.3)	NA	NS
EF min, %		58 (46-62)	61 (58-66)	NA	NS
Laboratory data	WBC, 10^3/uL	6.5 (5.0-11.1)	18.4 (12.3-20.7)	NA	0.048
	PLT, 10^3/mm^3	140 (93-221)	358 (181-361)	NA	NS
	ESR, mm/h	44 (36.5-53.5)	48 (42-58)	NA	NS
	CRP, mg/dL	21.3 (20.3-26.5)	7.0 (4.8-8.8)	NA	0.048
	Troponin max, ng/mL	0.050 (0.015-0.225)	ND	NA	NA

*1: median (Interquartile range (IQR)) unless specified. *2: Illness Day 1= first day of fever. *3: Maximum Z score (internal diameter normalized for body surface area) for the right and left anterior descending coronary arteries. *4: Late convalescent sera (illness day 414-990 days) from healthy children with a remote history of KD and with always normal coronary arteries by echocardiography, *5: p-values calculated by Mann-Whitney test for continuous variables between two groups (MIS-C vs KD) and Fisher's exact test for categorical variables. AA: African American, EFmin: the lowest ejection fraction (EF) level during hospitalization, WBC: white blood cell count, PLT: platelet count, ESR: erythrocyte sedimentation rate, CRP: C-reactive protein, Troponin max: the highest troponin level during hospitalization. ND: not done, NA: not applicable, NS: not significant

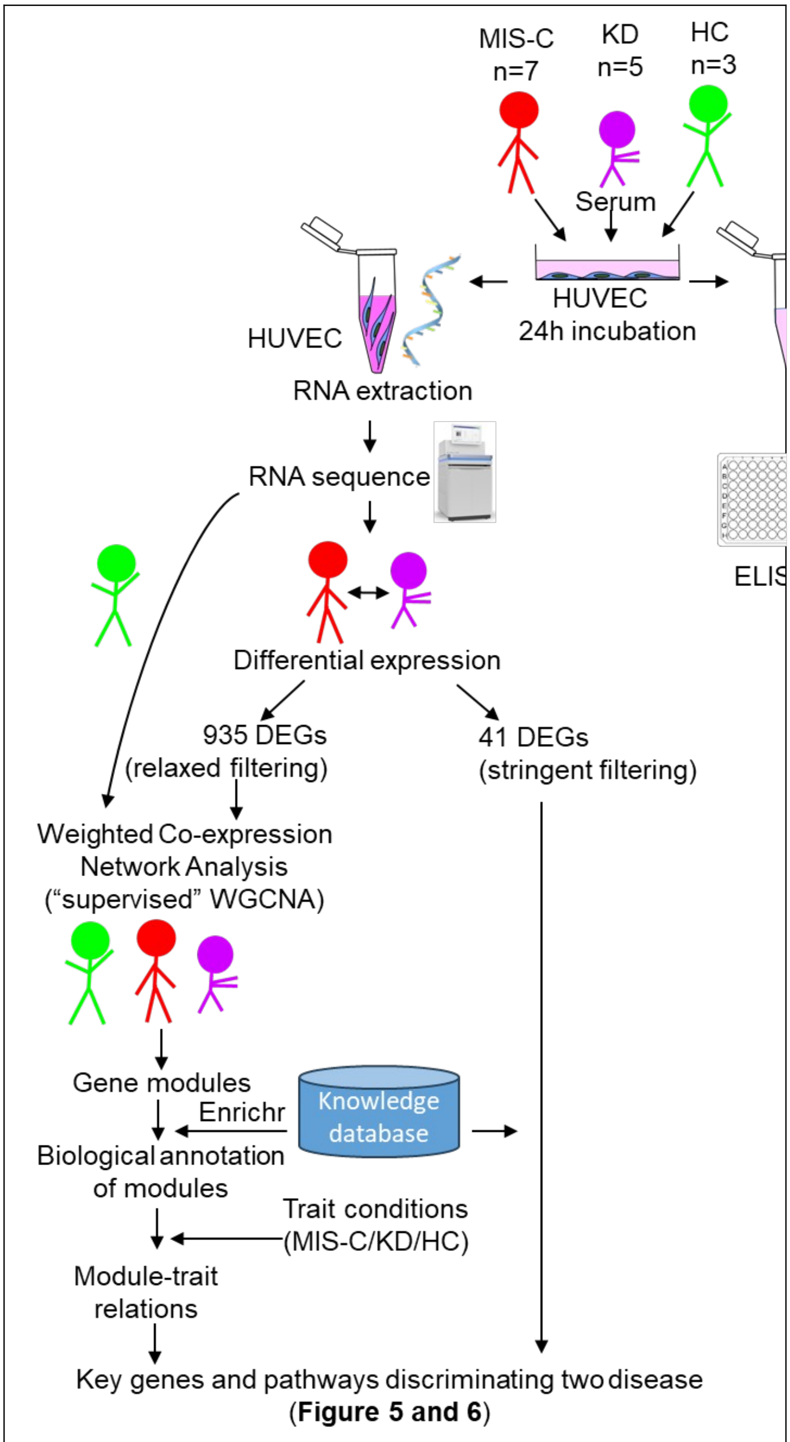

Figure 1. Work flow for EC study.
After human umbilical vein endothelial cells (HUVEC) were incubated with sera for 24 hours, RNA was extracted from cell lysates followed by RNAseq, differential expression analysis, and Weighted Gene Co-expression Network Analysis (WGCNA). Cell culture media from the same experiment were used for ELISA. DEG: differentially expressed genes, Enrichr: gene enrichment analysis (https://maayanlab.cloud/Enrichr/)

The first two principal components (PCs) of RNA-seq data showed clear separation of the three experimental groups with the healthy control samples in distinguishable from the no-sera samples (**Figure 2A**).

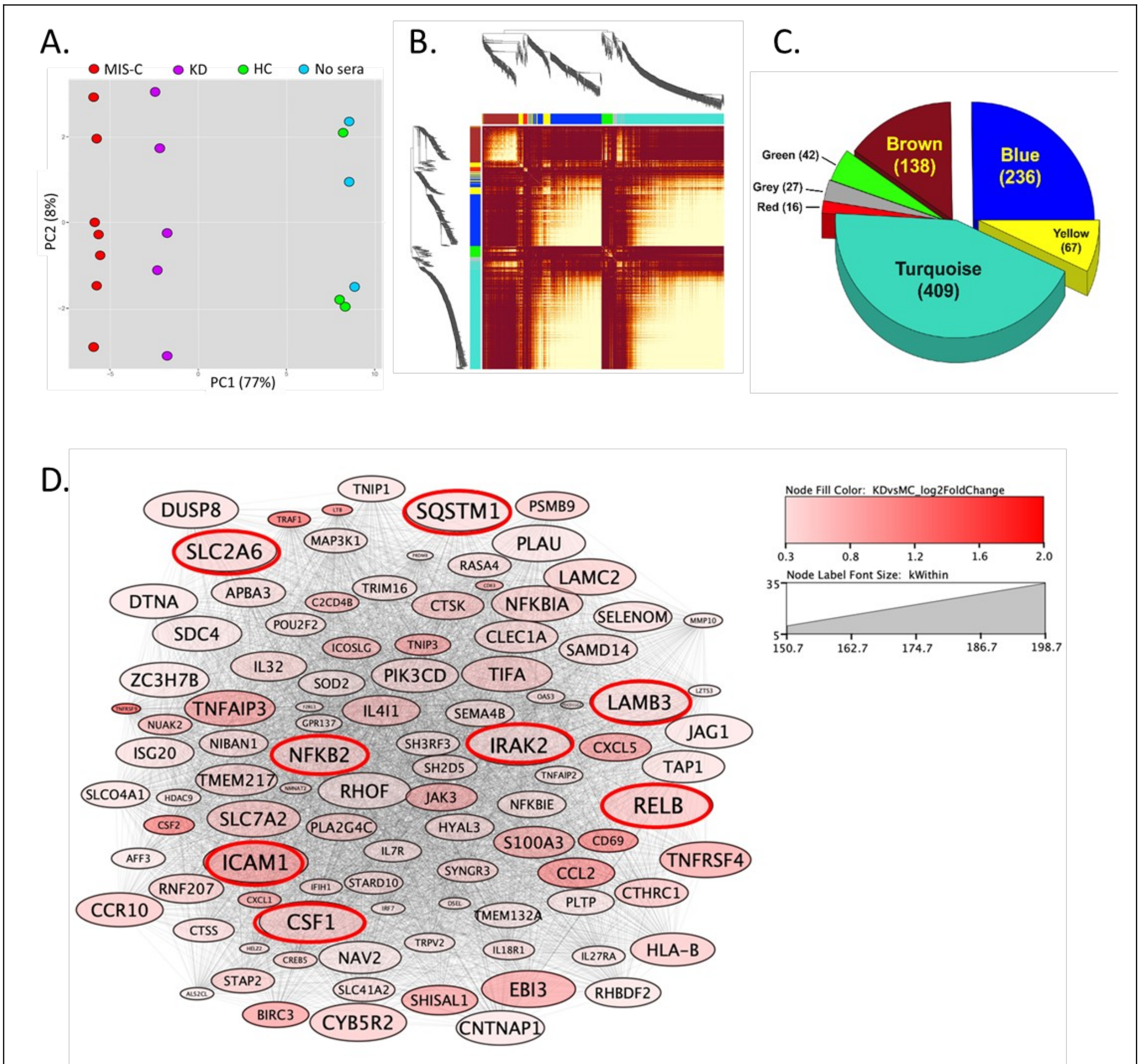

Figure 2. Factor analysis of transcript abundance in cultured ECs incubated with pre-treatment sera from KD, MIS-C, and HC. A: Plot of the first two principal components, B: Pearson correlations between expression profiles of 935 differentially expressed genes (DEGs) between MIS-C and KD with relaxed filter (fold change > 1.1 or <-1.1, un-adjusted p-value < 0.05, and count ≥ 10). C: Seven modules were identified with Weighted Gene Co-expression Network analysis (WGCNA). D: Network analysis was performed using the genes in the turquoise module. Eight of the top 10 hub genes (cut-off level: P-value of turquoise module membership < 0.05; intramodular connectivity (kWithin)>150; Adjacency > 0.2) are shown in red circles.

2.2. Weighted Gene Co-expression Analysis (WGCNA)

The gene co-expression network was constructed with 935 differentially expressed genes (DEGs) between KD and MIS-C partitioned into seven gene modules. Each module was labeled with a unique color name, with the grey color module as the least connected genes following the WGCNA color scheme. The topological overlap matrix (TOM~~P~~) plot (**Figure 2B**) shows the interconnectivity pattern among seven modules. The rows and columns of the TOM~~P~~ plot are genes, ~~and~~ the modules corresponded to blocks of highly connected genes, and ~~with~~ the darker red color cells in the TOM plot represent ~~the~~ higher interconnectedness. The three largest modules were turquoise > blue > brown (**Figure 2C**). To annotate biological meaning in each module, all genes in each module were used to identify the enriched pathways (https://maayanlab.cloud/Enrichr/) (**Table S1**) and the top 10 hub genes with the highest intramodular connectivity (kWithin) (**Table S2**) were selected. Based on these knowledge and data driven findings, we annotated a biological function to each module (**Figure 3A**).

The largest module (turquois, **Figure 3B**) was annotated as the "TNFα/NFκB" pathway and its top 10 hub genes included *RELB proto-oncogene, Nuclear factor kappa B (NFκB) subunit* (*RELB*), *sequestosome 1* (*SQSTM1*), and *Nuclear factor kappa B subunit 1* (*NFKB1*) (**Table S2**). Many turquoise module genes belonged to TNFα and IL1 pathways from the knowledgebased analysis and corresponded to the top hub genes from the data-driven network, since NFκB is the main downstream pathway regulated by TNFα and IL1 (**Figure 2D**).

The second largest module (blue) was annotated as EC homeostasis. The hub genes of the blue module included *endomucin* (*EMCN*), *RUNX1 partner transcriptional co-repressor 1* (*RUNX1T1*), *nuclear factor I A* (*NFIA*), and *nuclear factor I B* (*NFIB*). The key genes in the enriched pathways for the blue module were Brain Derived Neurotrophic Factor (BDNF) signaling pathway and NOS3 related pathways (**Table S1**). NOS3 is the enzyme that synthesizes nitric oxide, the key molecule that maintains endothelial cell homeostasis. Its expression is tightly regulated by many transcription factors and molecules including Nuclear Factor (NF)-1, the protein product of *NFIA* or *NFIB*, and glucocorticoids [11, 12]. Vascular endothelial growth factor (VEGF) also synthesizes nitric oxide through eNOS activation [13] and EMCN, RUNX1T1 and BDNF modify VEGF receptor pathway [14-18].

The third largest module (brown) had several ribosomal proteins genes (*RPL27, RPL6, and RPS23*) as hub genes and was enriched with molecules in the translation pathway.

Despite the smallest number of genes, the red module had important hub genes and enriched pathways, including glucocorticoid (GC) responsive genes and EndoMT suppression. Its hub genes included several GC regulated genes such as *hes family bHLH transcription factor 1* (*HES1*), *KLF transcription factor 10* (*KLF10*), *snail family transcriptional repressor 1* (*SNAI1*) and *growth arrest and DNA damage inducible beta* (*GADD45B*) [19-22]. HES1 is a master regulator of glucocorticoid receptor-dependent gene expression. The apparent mutual antagonism of HES1 and glucocorticoid (GC) receptor (GR) were reported [19]. SNAI is a key transcription factor to induce EndoMT through BDNF-TrkB pathway [21].

The yellow module had no strongly enriched pathway with adjp<1E-03. Its hub genes included anti-inflammatory genes such as *peroxiredoxin like 2A* (*PRXL2A*) [23] and *myocyte enhancer factor 2C* (*MEF2C*) [24] and gene related to immune response such as *lymphatic vessel endothelial hyaluronan receptor 1* (*LYVE1*) [25]. This module also include the hub genes, *calcitonin receptor like receptor* (*CALCRL*) [26], whose expression is regulated by GC and MEF2C [27], which co-operate with GC bound to GR to regulate gene expression. Therefore, this module may also have some connection with GC regulation. Similarly, the green and grey modules had no ~~a~~ significant pathway with p<1E-03. The hub genes in the green module included genes related to DNA repair such as *X-ray repair cross complementing 3* (*XRCC3*) [28] and *paired immunoglobin like type 2 receptor beta* (*PILRB*) [29]. The hub genes in the green module included apoptosis related genes, *zinc finger protein 428* (*ZNF428*) [30] and *modulator of apoptosis 1* (*MOAP1*) [31].

After annotating the biological meaning ~~at for~~of each module, we further assessed module-module relations (**Figure 3C**) and module-trait relations (**Figure 3B**). For each module, boxplots by trait were created using the values of the module eigengene (**Figure 3A**), the first principal component of -the expression matrix of the corresponding module~~member genes as a linear combination~~. While the turquoise module genes were up in MIS-C (**Figure 3B**), the blue module genes were down in MIS-C. This opposite signal is reflected in the strong negative module-module correlation between turquois and blue. The brown module genes were lower in MIS-C compared to KD.

The seven annotated modules were linked together visually to elucidate the contrasting underlying pathogeneses of two diseases (**Figure 3A**).

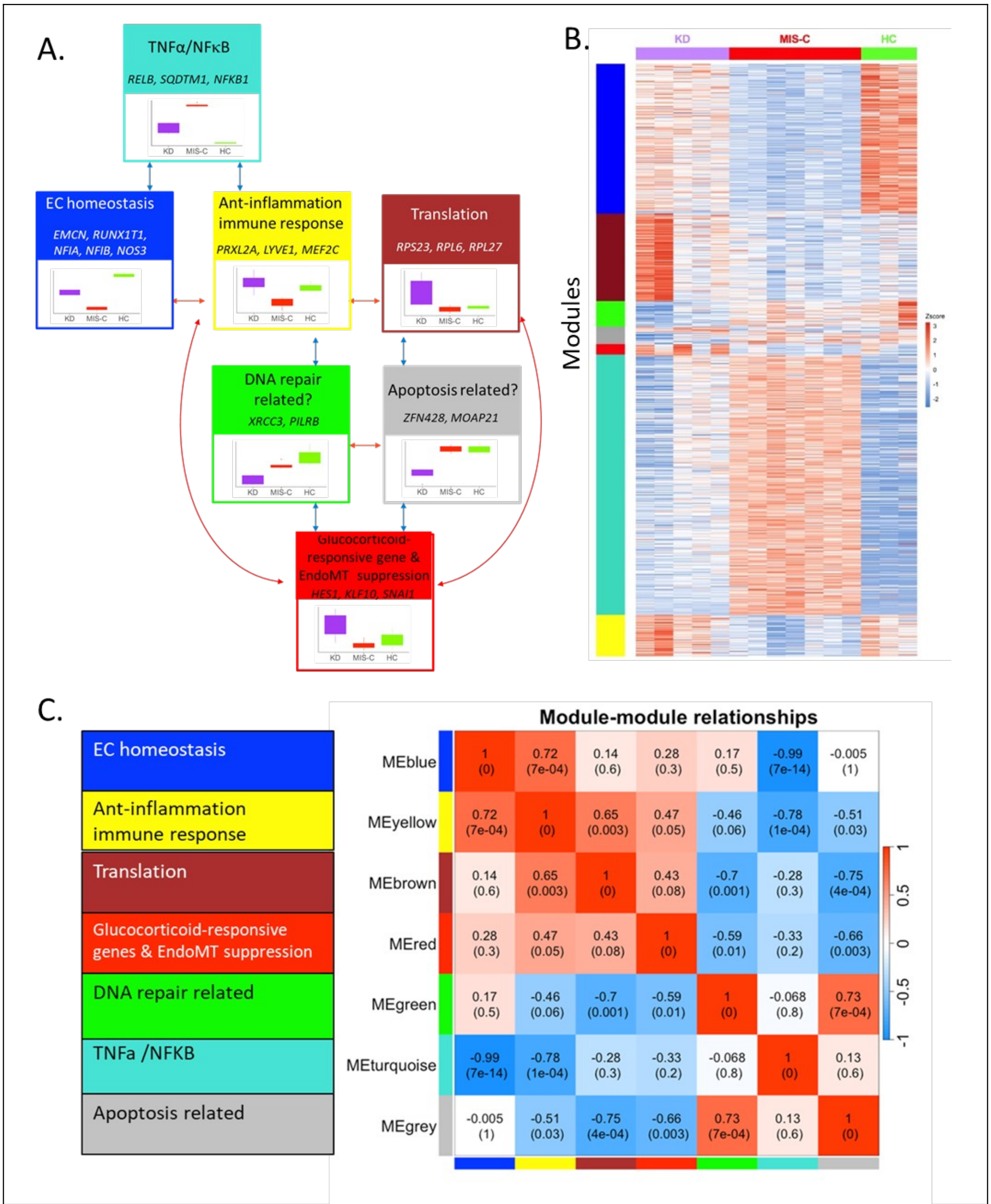

Figure 3. Annotated biological function, correlation, and expression pattern of seven modules in WGCNA A: Annotation of biological functions shown in top of each colored box. Genes represent key molecules found by pathway analysis or hub genes. The box plot in each colored box shows the levels of eigengene (Y-axis) from each cultured EC sample incubated with sera from KD, MIS-C, and HC. B: ~~Supervised H~~Heatmap of 935 transcripts by seven color-coded modules. C: Module-module correlation plot of eigengenes

2.3. Differential expression analysis with rigorous filter

Next, to directly identify differences in the EC response between MIS-C and KD, a rigorous filter (MIS-C vs. KD fold difference>2, adj p<0.05) was applied. Comparison of transcript abundance in ECs incubated with sera from KD and MIS-C patients revealed only 41 DEGs. The most significant DEG between KD and MIS-C was CCL2 (2.6 fold-increase in MIS-C, p=7.4E-126) (**Figure 4A**). Since CCL2 is secreted, CCL2 protein levels were measured in the media in which ECs were cultured. Although CCL2 transcript levels were very high in MIS-C compared to KD and HC, the secreted protein levels were not significantly different (**Figure S1**).

Of the 41 DEGs, 31 (76%) belonged to the turquoise module (Figure 4B) and included *TNF receptor associated factor 1* (*TRAF1*), *baculoviral IAP repeat containing 3* (*BIRC3*), *TNFRSF4 and 9*, *TNF alpha induced protein 3* (*TNFAIP3*), *TNFAIP3 interacting protein 3* (*TNIP3*), and *lymphotoxin beta* (*LTB*). Other turquoise module genes included NFκB-regulated chemokine genes (*CXCL1, 2, 3, 5, 6, CCL2*, and *20*) and the adhesion molecules *intercellular adhesion molecule 1* (*ICAM1*), *vascular cell adhesion molecule 1* (*VCAM1*), *ADAM metallopeptidase domain 8* (*ADAM8*), and *selectin E* (*SELE*). All of these genes were upregulated in MIS-C compared to KD. Three molecules (**Figure 4B**, underlined genes) in the turquoise module were reported to bind to SQSTM1, the second top hub gene of the turquoise module (**Figure 2D** and **Table S2**). These genes included *Epstein-Barr virus induced 3* (*EBI3*), and *ubiquitin D* (*UBD*), which are important in autophagy. Because expression of genes in the NFκB pathway inhibits apoptosis by stimulating expression of anti-apoptotic genes, we investigated whether the 41 DEGs were related to apoptosis. We found nine upregulated anti-apoptosis (pro-survival) genes and one downregulated pro-apoptosis gene (*Insulin like growth factor binding protein 5* (*IGFBP5*)) in MIS-C compared to KD (**Figure 4B,** blue and red arrows).

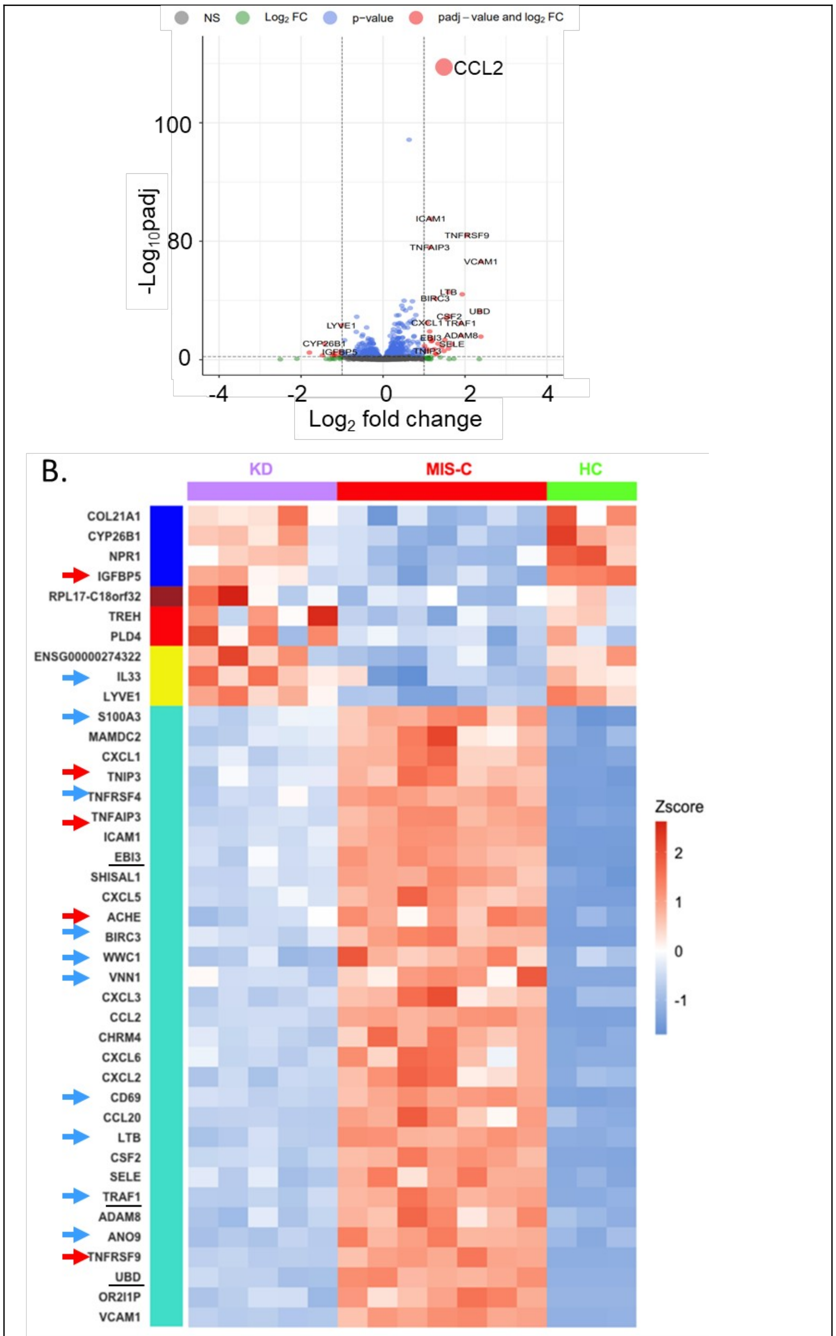

Figure 4. Differentially expressed genes (log_2 fold difference >1 and adj p<0.05) between ECs incubated with sera from MIS-C and KD. A: Volcano plot showing differential abundance of transcripts in ECs based on fold-difference in log2 scale and adjusted p-values. Compared to KD, transcripts to the left of the dotted vertical line were less abundant in ECs incubated with sera from MIS-C patients, while those to the right were more abundant. B: KD vs. MIS-C heatmap with 41 differentially expressed genes (DEGs) using KD (n=5, top purple bar), MIS-C (n=7, top red bar) and HC (n=3, top green bar). The color bars to the left of heatmap (blue, brown, red, yellow and turquoise) represent the gene modules classified by WGCNA. The genes with the arrows have pro-apoptotic (red) or anti-apoptotic (blue) effects. The genes with underline bind to SQSTM1.

These~~He~~ 41 DEGs also included genes in the blue module (EC homeostasis), brown module (translation), red (glucocorticoids responsive gene and EndoMT suppression), and yellow (anti-inflammation and immune response), all of which fit the biological functions annotated by WGCNA (**Figure 5**).

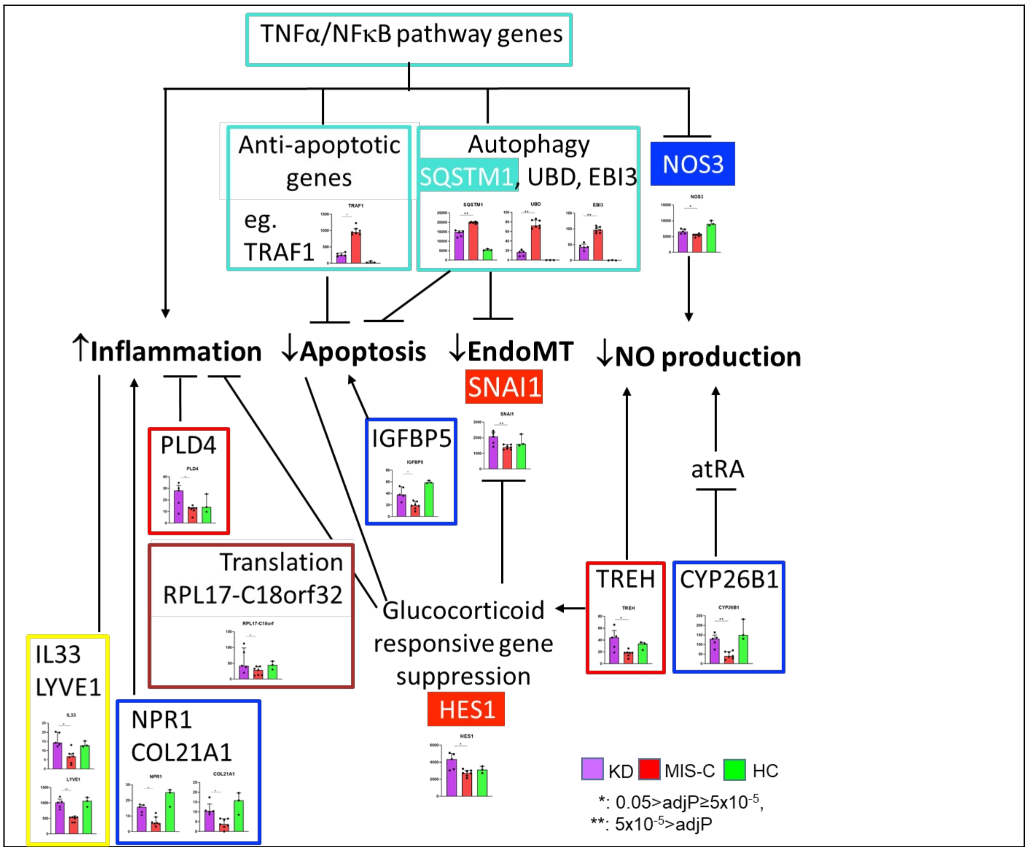

Figure 5. Suggested biological meaning at the intersection of the gene modules from network analysis and 41 DEGs between MIS-C and KD.
Color-coded boxes represent the gene modules from WGCNA. Genes in filled boxes were not among the 41 DEGs but are key molecules in the WGCNA modules. SQSMT1, UBD and EBI3 have important roles in protein degradation [32, 33] and SQSTM1-dependent degradation of snail (SNAI1), a transcription factor regulating EndoMT, has been reported [34]. *Cytochrome P450 family 26 subfamily B member 1* (*CYP26B1*) and *trehalase* (*TREH*) are genes that influence NO production in ECs [35, 36]. TREH also induces functional confirmation in glucocorticoid receptor [37]. IGFBP5 relates to apoptosis [38]. Relation with inflammation was reported for PLD4 [39], NPR1 [40], COL21A1 [41], IL33 [42] and LYVE1 [25]. The effects of IL-33 are either pro- or anti-inflammatory depending on the disease. LYVE1 is important for leukocyte trafficking. Post-transcriptional regulation of CCL2 by GC is well reported [43]. GC binds to GC receptor (GR) in the cytosol and exerts its anti-inflammatory functions by inhibiting expression of cytokines, chemokines and adhesion molecules in ECs [44]. GC has tissue specific action on apoptosis[45]. GC inhibit protein synthesis by inhibiting translation initiation and ribosomal synthesis at the level of transcription, posttranscription and translation [46-48]. *RPL17-C18orf32* is read-through transcript between *RPL17* (*ribosomal protein L17*) and *C18orf32* (*chromosome 18 open reading frame 32*) genes.

3. Discussion

The response of cultured ECs to incubation with acute, pre-treatment sera from KD and MIS-C patients differed significantly. ECs incubated with MIS-C sera expressed higher levels of transcripts associated with cell survival and lower levels of transcripts associated with EndoMT when compared to KD. ECs incubated with MIS-C sera had depressed levels of transcripts that are modulated by GC compared to KD, suggesting increased serum GC levels in MIS-C. These differences may influence the divergent cardiovascular outcomes in the two diseases (**Figure 5**).

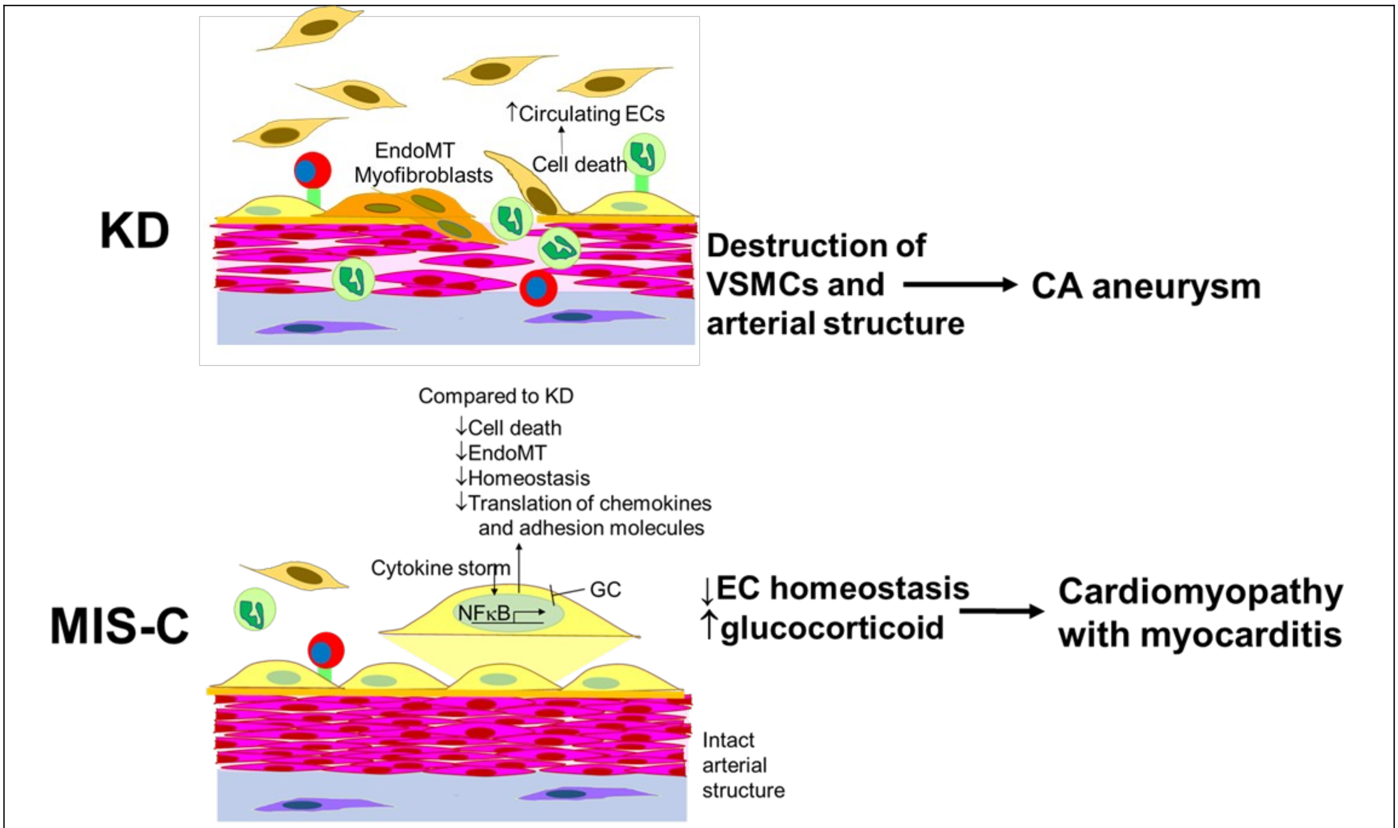

Figure 6. Proposed model of EC response in patients with KD and MIS-C
ECs in MIS-C are more likely to survive and less likely to undergo EndoMT. However, their reduced expression of genes mediating EC homeostasis and increased influence GC may lead to transient LV dysfunction in MIS-C (MIS-C cardiomyopathy/myocarditis) by analogy to Takotsubo syndrome [49]. Although ECs in MIS-C had higher transcript levels of adhesion molecules and chemokines, those protein expression on the membrane and secretion may be limited and the endothelium remains intact. Contrastingly, in KD, more ECs may undergo apoptosis and shed into the circulation or undergo EndoMT and promote destruction of the vascular wall [50]. Yellow cells: endothelial cells (ECs), Brown cells: circulating ECs, Orange cells: myofibroblasts, Pink cells: smooth muscle cells, Purple cells: fibroblasts, Green cells: neutrophils, Red cells: monocytes

Activation of the NFκB pathway was ~~a key pathway~~critical in the EC response in MIS-C patients. NF-κB regulates transcription of many proinflammatory and pro-survival genes. We found nine up-regulated pro-survival genes in MIS-C compared to KD including *S100A3* [51], *TNFRSF4* [52], *BIRC3* [53], *WWC1* [54], *VNN1* [55], *CD69* [56], *LTB* [57], *TRAF1* [58], and *ANO9* [59]. We also found that an independent pro-apoptotic gene, *IGFBP5* [60], was downregulated in MIS-C. Taken together, these findings suggest that ECs in MIS-C have a more pro-survival phenotype compared to KD. These findings are consistent with the report that circulating endothelial cells (CECs) were released into the blood in 100% of acute KD patients but in only 26% of acute MIS-C patients compared to normal controls [50].

SQSTM1, also known as p62, is one of the key proteins induced by NFkB. SQSTM1 is a scaffold protein with multiple domains, which allows it to bind multiple proteins. By binding different molecules through theses domains, SQSTM1 has pleiotropic effects including activation of the NFκB pathway and mediating protein degradation (ubiquitin–proteasome system and autophagy), cell death, and cell survival depending on the binding proteins [61]. SQSTM1 and autophagy influence EndoMT, the process that transforms ECs into myofibroblasts [34, 62]. Myofibroblasts clearly play a role in damaging the coronary arteries in KD [63, 64].

Nitric oxide (NO) is a critical molecule in the maintenance of endothelial cell homeostasis and regulation of vascular tone and permeability. Therefore, NO bioavailability is tightly regulated by NO synthases, especially NOS3 in ECs. TREH, CYP26B1 and GC also regulate NO syntheses. Overall, we found lower transcript levels of genes that regulate NO levels in MIS-C. Abnormal EC homeostasis may be more severe in MIS-C compared to KD and may lead to myocardial stunning [49, 65]. Takotsubo cardiomyopathy, a transient left ventricular dysfunction that spontaneously recovers within days, may be a model for the myocardial dysfunction in MIS-C [49]. Of interest, genetic variants in BAG cochaperone 3 (BAG3), which has an important role in autophagy through binding to SQSTM1, have been associated with Takotsubo cardiomyopathy [66]. GC also induce vasospastic angina with elevated ST segments by affecting ECs [67]. GC decreases intracellular calcium mobilization, NOS3, and, nitric oxide in ECs [12, 68]. GC also suppresses the production of the vasodilator, prostacyclin, and increases the synthesis of the vasoconstrictor, thromboxane [69]. Abnormal EC homeostasis and GC-induced constriction could lead to reduced blood flow in the heart contributing to myocardial dysfunction. LV dysfunction is a prominent feature of MIS-C [70-73]. The degree of endothelial dysfunction based on the studies of flow-mediated dilation of brachial arteries correlated with arterial stiffness and reduced ejection fractions in MIS-C [74].

GC-bound GR inhibit the expression of inflammatory molecules on the EC surface such as adhesion molecules, SELE and VCAM-1, and secretion of chemokines including CCL2 [44]. GCs control gene expression through transcriptional and post-transcriptional regulation. GC inhibit protein synthesis by inhibiting translation initiation and ribosomal synthesis at the level of transcription, posttranscription and translation [46-48]. Translation initiation machinery includes many molecules including EIF3, RPS6 kinase, ribosomes that are composed of ribosomal RNA and ribosomal proteins (ribosome 40S containing 18S rRNA and 33 ribosomal proteins (RPS) and ribosome 60S containing three rRNAs (25S, 5.8S, 5S) and 49 ribosomal proteins (RPL)) [47, 75, 76]. Transcript levels of many of these ribosomal proteins were reduced in MIS-C compared to KD.

Limitations

In our descriptive study of the EC response *ex vivo* to sera from MIS-C and KD patients, we only characterized the transcriptome and not the translation of key transcripts into protein except for CCL2 that was translated and secreted in the media. Limitations in availability of pre-treatment patient sera precluded more extensive analyses. We justified the use of HUVECs instead of coronary artery EC based on previous work by our group showing similar responses of these two cell lines.[77] However, it is possible that the responses could be different in this experimental model. Comparison of blood levels of GC between the patients is difficult since GC levels require standardized, timed blood samples that were not available before treatment.

Conclusion

This *ex vivo* model allowed insight into disease pathogenesis in an otherwise clinically inaccessible tissue. ECs incubated with pre-treatment sera from patients with KD and MIS-C showed important differences in the transcriptional response. Compared to KD, ECs incubated with MIS-C sera expressed genes favoring cell survival. However, the suppression of genes supporting EC homeostasis and increased serum GC levels in the patients with MIS-C may contribute to the transient and quickly reversible myocardial dysfunction that is common in MIS-C patients. ECs incubated with KD sera upregulated genes associated with EndoMT. These transcriptional differences support the clinically observed differences in cardiovascular outcome in the two diseases.

4. Materials and Methods

Patients and samples

The demographic and clinical characteristics of study patients are presented in **Table 1**. All patients with KD and MIS-C were diagnosed by one of two clinicians specializing in KD and MIS-C (JCB and AHT) at Rady Children's Hospital San Diego and met the American Heart Association criteria for complete KD or CDC criteria for MIS-C [78, 79]. In order to avoid the potential for misclassification, all MIS-C patients had positive antibody testing for the nucleocapsid protein of SARS-CoV-2 and none had received a SARS-CoV-2 vaccine. Serum samples were collected prior to treatment from patients with KD (illness day 4-7), and MIS-C (illness day 2-8). Late convalescent (illness day 414-990 days) sera from KD with a remote history of KD and with always normal coronary arteries by echocardiography served as healthy controls.

Cell culture

Detailed methods were as previously described [10]. In the experiments involving patients' sera, M199 was supplemented with 10% patient serum (individual) and 2% fetal bovine serum (FBS) (100μL patient serum, 20μL FBS and 880μL medium per well of a six-well plate)**.** For RNA sequencing (RNA-seq), human umbilical vein ECs (HUVECs) were incubated without or with individual, pre-treatment sera from KD patients, MIS-C patients and HC for 24hr.

RNA extraction, RNA sequencing and RT-PCR

Total RNA from HUVECs was isolated using miRVana (ThermoFisher) for RNA-seq. For RNA-seq analysis, RNA sequencing libraries were generated using the Illumina Ribo-Zero Plus rRNA Depletion Kit with IDT for Illumina RNA UD Indexes (Illumina, San Diego, CA). Samples were processed following manufacturer's instructions. Resulting libraries were multiplexed and sequenced with 100 basepair (bp) Paired End (PE100) reads to a depth of approximately 25 per million reads on an Illumina NovaSeq 6000. Samples were demultiplexed using bcl2fastq v2.20 Conversion Software (Illumina, San Diego, CA).

Differential expression analysis

The RNA-Seq analysis pipeline consisted of the following steps: quality control using fastp [80] and MultiQC [81], quantification using salmon [82], and differential expression analysis using DESeq2 [83]. R version 4.3.4 and Python version 3.8.5 were used in data analysis, file management, and visualization. The cutoff value of the adjusted p-value (Benjamini-Hochberg method) for multiple testing was predefined as 0.05. The minimum required absolute fold change was set as 1.25 in log2-scale. All computation was conducted in Amazon Elastic Computing (EC2) instances, the virtual servers in the cloud computing environment. A heatmap was generated after applying hierarchical clustering on the normalized gene expression values with Euclidean distance and complete-linkage.

Weighted gene correlation network analysis (WGCNA) Analysis

We performed a ~~un~~supervised WGCNA on non-normalized RNAseq data from all subjects. Genes with raw counts less than 10 in all phenotypic groups (KD, MIS-C and HC) were excluded. The one-step automatic network construction and module detection was used based on a soft power of 12 and signed topological overlap matrices. The gene expression profile of a module was summarized by module eigengene, which is defined as the principal component of the module. All genes were univocally assigned to a single module based on quantified module membership of intramodular connectivity. The analysis was computed using the R package *WGCNA* v1.72 [84].

Statistical Analysis

Values were expressed as medians and interquartile ranges. Mann–Whitney *U* test or Kruskal-Wallis was used to analyze differences among indicated groups. $P<0.05$ was considered statistically significant.

Supplementary Materials: The following supporting information can be downloaded at: www.mdpi.com/xxx/s1, Figure S1: CCL2 transcript and protein levels; Table S1: Differential expression analysis results (excel file); Table S2: Top three significant pathways (adjusted p<0.001) for seven module in WGCNA, Table S3: Top 10 hub genes for seven modules in WGCNA.

Author Contributions: Conceptualization, JK, CS, JS and JB; Methodology, JK, CS, MH and HW; Formal analysis, JK, CS and HW; Investigation, CS; Data curation, JK, CS; Writing – original draft, JK, , CS, HW; Writing – review & editing, MH, AT,JB, JS; Visualization, JK, CS, HW; Supervision, JK, JS, JB; Funding acquisition, HH, AT, JS, JB.

Funding: This work was supported in part by grants from the National Institutes of Health (R01HL140898 to JCB, AHT, JYS, and HMH), and the Gordon and Marilyn Macklin Foundation. This publication includes RNA sequence data generated at the UC San Diego IGM Genomics Center utilizing an Illumina NOVASeq 6000 that was purchased with funding from a National Institutes of Health SIG grant (#S10 OD026929).

Institutional Review Board Statement: The Human Research Protection Program of the University of California San Diego approved this research protocol (UCSD # 140220 and #200977).

Informed Consent Statement: Written informed consent and assent was obtained from the parents and patients as appropriate.

Data Availability Statement: The RNA-Seq data generated during the current study are publicly available in the NCBI GEO with accession number ~~GSEXXXX~~ GSE236833.~~(Accession number will be available upon the completion of GEO review) (https://www.ncbi.nlm.nih.gov/geo/query/acc.cgi?acc=GSEXXXX)~~

Acknowledgments: We thank Joan Pancheri, RN, and Ellie Moreno for patient sample collection and laboratory assistance, and Emelia Bainto and Nipha Sivilay for patient data collection.

Disclosures: None

References

1. Whittaker, E.; Bamford, A.; Kenny, J.; Kaforou, M.; Jones, C. E.; Shah, P.; Ramnarayan, P.; Fraisse, A.; Miller, O.; Davies, P.; Kucera, F.; Brierley, J.; McDougall, M.; Carter, M.; Tremoulet, A.; Shimizu, C.; Herberg, J.; Burns, J. C.; Lyall, H.; Levin, M.; Group, P.-T. S.; Euclids; Consortia, P., Clinical Characteristics of 58 Children With a Pediatric Inflammatory Multisystem Syndrome Temporally Associated With SARS-CoV-2. *JAMA* **2020**.
2. Lam, J. Y.; Shimizu, C.; Tremoulet, A. H.; Bainto, E.; Roberts, S. C.; Sivilay, N.; Gardiner, M. A.; Kanegaye, J. T.; Hogan, A. H.; Salazar, J. C.; Mohandas, S.; Szmuszkovicz, J. R.; Mahanta, S.; Dionne, A.; Newburger, J. W.; Ansusinha, E.; DeBiasi, R. L.; Hao, S.; Ling, X. B.; Cohen, H. J.; Nemati, S.; Burns, J. C.; Pediatric Emergency Medicine Kawasaki Disease Research, G.; Group, C. S., A machine-learning algorithm for diagnosis of multisystem inflammatory syndrome in children and Kawasaki disease in the USA: a retrospective model development and validation study. *Lancet Digit Health* **2022,** 4, (10), e717-e726.
3. Skochko, S. M.; Jain, S.; Sun, X.; Sivilay, N.; Kanegaye, J. T.; Pancheri, J.; Shimizu, C.; Sheets, R.; Tremoulet, A. H.; Burns, J. C., Kawasaki Disease Outcomes and Response to Therapy in a Multiethnic Community: A 10-Year Experience. *J. Pediatr.* **2018,** 203, 408-415 e3.
4. Newburger, J. W.; Takahashi, M.; Beiser, A. S.; Burns, J. C.; Bastian, J.; Chung, K. J.; Colan, S. D.; Duffy, C. E.; Fulton, D. R.; Glode, M. P.; et al., A single intravenous infusion of gamma globulin as compared with four infusions in the treatment of acute Kawasaki syndrome. *N. Engl. J. Med.* **1991,** 324, (23), 1633-9.
5. Son, M. B. F.; Murray, N.; Friedman, K.; Young, C. C.; Newhams, M. M.; Feldstein, L. R.; Loftis, L. L.; Tarquinio, K. M.; Singh, A. R.; Heidemann, S. M.; Soma, V. L.; Riggs, B. J.; Fitzgerald, J. C.; Kong, M.; Doymaz, S.; Giuliano, J. S., Jr.; Keenaghan, M. A.; Hume, J. R.; Hobbs, C. V.; Schuster, J. E.; Clouser, K. N.; Hall, M. W.; Smith, L. S.; Horwitz, S. M.; Schwartz, S. P.; Irby, K.; Bradford, T. T.; Maddux, A. B.; Babbitt, C. J.; Rowan, C. M.; McLaughlin, G. E.; Yager, P. H.; Maamari, M.; Mack, E. H.; Carroll, C. L.; Montgomery, V. L.; Halasa, N. B.; Cvijanovich, N. Z.; Coates, B. M.; Rose, C. E.; Newburger, J. W.; Patel, M. M.; Randolph, A. G.; Overcoming, C.-I., Multisystem Inflammatory Syndrome in Children - Initial Therapy and Outcomes. *N. Engl. J. Med.* **2021,** 385, (1), 23-34.
6. Alsaied, T.; Tremoulet, A. H.; Burns, J. C.; Saidi, A.; Dionne, A.; Lang, S. M.; Newburger, J. W.; de Ferranti, S.; Friedman, K. G., Review of Cardiac Involvement in Multisystem Inflammatory Syndrome in Children. *Circulation* **2021,** 143, (1), 78-88.
7. Mayordomo-Colunga, J.; Vivanco-Allende, A.; Lopez-Alonso, I.; Lopez-Martinez, C.; Fernandez-Vega, I.; Gil-Pena, H.; Rey, C., SARS-CoV-2 Spike Protein in Intestinal Cells of a Patient with Coronavirus Disease 2019 Multisystem Inflammatory Syndrome. *J. Pediatr.* **2022,** 243, 214-218 e5.
8. Duarte-Neto, A. N.; Caldini, E. G.; Gomes-Gouvea, M. S.; Kanamura, C. T.; de Almeida Monteiro, R. A.; Ferranti, J. F.; Ventura, A. M. C.; Regalio, F. A.; Fiorenzano, D. M.; Gibelli, M.; Carvalho, W. B.; Leal, G. N.; Pinho, J. R. R.; Delgado, A. F.; Carneiro-Sampaio, M.; Mauad, T.; Ferraz da Silva, L. F.; Saldiva, P. H. N.; Dolhnikoff, M., An autopsy study of the spectrum of severe COVID-19 in children: From SARS to different phenotypes of MIS-C. *EClinicalMedicine* **2021,** 35, 100850.
9. Ghosh, P.; Katkar, G. D.; Shimizu, C.; Kim, J.; Khandelwal, S.; Tremoulet, A. H.; Kanegaye, J. T.; Pediatric Emergency Medicine Kawasaki Disease Research, G.; Bocchini, J.; Das, S.; Burns, J. C.; Sahoo, D., An Artificial Intelligence-guided signature reveals the shared host immune response in MIS-C and Kawasaki disease. *Nat Commun* **2022,** 13, (1), 2687.
10. He, M.; Chen, Z.; Martin, M.; Zhang, J.; Sangwung, P.; Woo, B.; Tremoulet, A. H.; Shimizu, C.; Jain, M. K.; Burns, J. C.; Shyy, J. Y., miR-483 Targeting of CTGF Suppresses Endothelial-to-Mesenchymal Transition: Therapeutic Implications in Kawasaki Disease. *Circ. Res.* **2017,** 120, (2), 354-365.
11. Qian, X. X.; Mata-Greenwood, E.; Liao, W. X.; Zhang, H.; Zheng, J.; Chen, D. B., Transcriptional regulation of endothelial nitric oxide synthase expression in uterine artery endothelial cells by c-Jun/AP-1. *Mol. Cell. Endocrinol.* **2007,** 279, (1-2), 39-51.
12. Wallerath, T.; Witte, K.; Schafer, S. C.; Schwarz, P. M.; Prellwitz, W.; Wohlfart, P.; Kleinert, H.; Lehr, H. A.; Lemmer, B.; Forstermann, U., Down-regulation of the expression of endothelial NO synthase is likely to contribute to glucocorticoid-mediated hypertension. *Proc. Natl. Acad. Sci. U. S. A.* **1999,** 96, (23), 13357-62.
13. Ahmad, S.; Hewett, P. W.; Wang, P.; Al-Ani, B.; Cudmore, M.; Fujisawa, T.; Haigh, J. J.; le Noble, F.; Wang, L.; Mukhopadhyay, D.; Ahmed, A., Direct evidence for endothelial vascular endothelial growth factor receptor-1 function in nitric oxide-mediated angiogenesis. *Circ. Res.* **2006,** 99, (7), 715-22.
14. Park-Windhol, C.; Ng, Y. S.; Yang, J.; Primo, V.; Saint-Geniez, M.; D'Amore, P. A., Endomucin inhibits VEGF-induced endothelial cell migration, growth, and morphogenesis by modulating VEGFR2 signaling. *Sci Rep* **2017,** 7, (1), 17138.
15. Liao, K. H.; Chang, S. J.; Chang, H. C.; Chien, C. L.; Huang, T. S.; Feng, T. C.; Lin, W. W.; Shih, C. C.; Yang, M. H.; Yang, S. H.; Lin, C. H.; Hwang, W. L.; Lee, O. K., Endothelial angiogenesis is directed by RUNX1T1-regulated VEGFA, BMP4 and TGF-beta2 expression. *PLoS One* **2017,** 12, (6), e0179758.
16. Baby, N.; Li, Y.; Ling, E. A.; Lu, J.; Dheen, S. T., Runx1t1 (Runt-related transcription factor 1; translocated to, 1) epigenetically regulates the proliferation and nitric oxide production of microglia. *PLoS One* **2014,** 9, (2), e89326.
17. Lin, C. Y.; Hung, S. Y.; Chen, H. T.; Tsou, H. K.; Fong, Y. C.; Wang, S. W.; Tang, C. H., Brain-derived neurotrophic factor increases vascular endothelial growth factor expression and enhances angiogenesis in human chondrosarcoma cells. *Biochem. Pharmacol.* **2014,** 91, (4), 522-33.
18. Zhang, Z.; Zhang, Y.; Zhou, Z.; Shi, H.; Qiu, X.; Xiong, J.; Chen, Y., BDNF regulates the expression and secretion of VEGF from osteoblasts via the TrkB/ERK1/2 signaling pathway during fracture healing. *Mol Med Rep* **2017,** 15, (3), 1362-1367.

19. Revollo, J. R.; Oakley, R. H.; Lu, N. Z.; Kadmiel, M.; Gandhavadi, M.; Cidlowski, J. A., HES1 is a master regulator of glucocorticoid receptor-dependent gene expression. *Sci Signal* **2013,** 6, (304), ra103.
20. Leclerc, N.; Luppen, C. A.; Ho, V. V.; Nagpal, S.; Hacia, J. G.; Smith, E.; Frenkel, B., Gene expression profiling of glucocorticoid-inhibited osteoblasts. *J. Mol. Endocrinol.* **2004,** 33, (1), 175-93.
21. Yang, H. W.; Lee, S. A.; Shin, J. M.; Park, I. H.; Lee, H. M., Glucocorticoids ameliorate TGF-beta1-mediated epithelial-to-mesenchymal transition of airway epithelium through MAPK and Snail/Slug signaling pathways. *Sci Rep* **2017,** 7, (1), 3486.
22. Mostafa, M. M.; Rider, C. F.; Shah, S.; Traves, S. L.; Gordon, P. M. K.; Miller-Larsson, A.; Leigh, R.; Newton, R., Glucocorticoid-driven transcriptomes in human airway epithelial cells: commonalities, differences and functional insight from cell lines and primary cells. *BMC Med Genomics* **2019,** 12, (1), 29.
23. He, H.; Guo, F.; Li, Y.; Saaoud, F.; Kimmis, B. D.; Sandhu, J.; Fan, M.; Maulik, D.; Lessner, S.; Papasian, C. J.; Fan, D.; Jiang, Z.; Fu, M., Adiporedoxin suppresses endothelial activation via inhibiting MAPK and NF-kappaB signaling. *Sci Rep* **2016,** 6, 38975.
24. Xu, Z.; Yoshida, T.; Wu, L.; Maiti, D.; Cebotaru, L.; Duh, E. J., Transcription factor MEF2C suppresses endothelial cell inflammation via regulation of NF-kappaB and KLF2. *J. Cell. Physiol.* **2015,** 230, (6), 1310-20.
25. Johnson, L. A.; Banerji, S.; Lawrance, W.; Gileadi, U.; Prota, G.; Holder, K. A.; Roshorm, Y. M.; Hanke, T.; Cerundolo, V.; Gale, N. W.; Jackson, D. G., Dendritic cells enter lymph vessels by hyaluronan-mediated docking to the endothelial receptor LYVE-1. *Nat Immunol* **2017,** 18, (7), 762-770.
26. Nikitenko, L. L.; Smith, D. M.; Bicknell, R.; Rees, M. C., Transcriptional regulation of the CRLR gene in human microvascular endothelial cells by hypoxia. *FASEB J.* **2003,** 17, (11), 1499-501.
27. Speksnijder, N.; Christensen, K. V.; Didriksen, M.; De Kloet, E. R.; Datson, N. A., Glucocorticoid receptor and myocyte enhancer factor 2 cooperate to regulate the expression of c-JUN in a neuronal context. *J. Mol. Neurosci.* **2012,** 48, (1), 209-18.
28. Pierce, A. J.; Johnson, R. D.; Thompson, L. H.; Jasin, M., XRCC3 promotes homology-directed repair of DNA damage in mammalian cells. *Genes Dev.* **1999,** 13, (20), 2633-8.
29. Du, W.; Amarachintha, S.; Wilson, A.; Pang, Q., The immune receptor Trem1 cooperates with diminished DNA damage response to induce preleukemic stem cell expansion. *Leukemia* **2017,** 31, (2), 423-433.
30. Camara-Quilez, M.; Barreiro-Alonso, A.; Vizoso-Vazquez, A.; Rodriguez-Belmonte, E.; Quindos-Varela, M.; Lamas-Maceiras, M.; Cerdan, M. E., The HMGB1-2 Ovarian Cancer Interactome. The Role of HMGB Proteins and Their Interacting Partners MIEN1 and NOP53 in Ovary Cancer and Drug-Response. *Cancers (Basel)* **2020,** 12, (9).
31. Tan, C. T.; Zhou, Q. L.; Su, Y. C.; Fu, N. Y.; Chang, H. C.; Tao, R. N.; Sukumaran, S. K.; Baksh, S.; Tan, Y. J.; Sabapathy, K.; Yu, C. D.; Yu, V. C., MOAP-1 Mediates Fas-Induced Apoptosis in Liver by Facilitating tBid Recruitment to Mitochondria. *Cell Rep* **2016,** 16, (1), 174-185.
32. Watanabe, A.; Mizoguchi, I.; Hasegawa, H.; Katahira, Y.; Inoue, S.; Sakamoto, E.; Furusaka, Y.; Sekine, A.; Miyakawa, S.; Murakami, F.; Xu, M.; Yoneto, T.; Yoshimoto, T., A Chaperone-Like Role for EBI3 in Collaboration With Calnexin Under Inflammatory Conditions. *Front Immunol* **2021,** 12, 757669.
33. Aichem, A.; Kalveram, B.; Spinnenhirn, V.; Kluge, K.; Catone, N.; Johansen, T.; Groettrup, M., The proteomic analysis of endogenous FAT10 substrates identifies p62/SQSTM1 as a substrate of FAT10ylation. *J. Cell Sci.* **2012,** 125, (Pt 19), 4576-85.
34. Grassi, G.; Di Caprio, G.; Santangelo, L.; Fimia, G. M.; Cozzolino, A. M.; Komatsu, M.; Ippolito, G.; Tripodi, M.; Alonzi, T., Autophagy regulates hepatocyte identity and epithelial-to-mesenchymal and mesenchymal-to-epithelial transitions promoting Snail degradation. *Cell Death Dis* **2015,** 6, (9), e1880.
35. Achan, V.; Tran, C. T.; Arrigoni, F.; Whitley, G. S.; Leiper, J. M.; Vallance, P., all-trans-Retinoic acid increases nitric oxide synthesis by endothelial cells: a role for the induction of dimethylarginine dimethylaminohydrolase. *Circ. Res.* **2002,** 90, (7), 764-9.
36. LaRocca, T. J.; Henson, G. D.; Thorburn, A.; Sindler, A. L.; Pierce, G. L.; Seals, D. R., Translational evidence that impaired autophagy contributes to arterial ageing. *J Physiol* **2012,** 590, (14), 3305-16.
37. Khan, S. H.; Arnott, J. A.; Kumar, R., Naturally occurring osmolyte, trehalose induces functional conformation in an intrinsically disordered activation domain of glucocorticoid receptor. *PLoS One* **2011,** 6, (5), e19689.
38. Qiao, D.; Xu, J.; Le, C.; Huang, E.; Liu, C.; Qiu, P.; Lin, Z.; Xie, W. B.; Wang, H., Insulin-like growth factor binding protein 5 (IGFBP5) mediates methamphetamine-induced dopaminergic neuron apoptosis. *Toxicol. Lett.* **2014,** 230, (3), 444-53.
39. Gavin, A. L.; Huang, D.; Blane, T. R.; Thinnes, T. C.; Murakami, Y.; Fukui, R.; Miyake, K.; Nemazee, D., Cleavage of DNA and RNA by PLD3 and PLD4 limits autoinflammatory triggering by multiple sensors. *Nat Commun* **2021,** 12, (1), 5874.
40. Gogulamudi, V. R.; Mani, I.; Subramanian, U.; Pandey, K. N., Genetic disruption of Npr1 depletes regulatory T cells and provokes high levels of proinflammatory cytokines and fibrosis in the kidneys of female mutant mice. *Am J Physiol Renal Physiol* **2019,** 316, (6), F1254-F1272.
41. Zhang, K.; Tao, C.; Xu, J.; Ruan, J.; Xia, J.; Zhu, W.; Xin, L.; Ye, H.; Xie, N.; Xia, B.; Li, C.; Wu, T.; Wang, Y.; Schroyen, M.; Xiao, X.; Fan, J.; Yang, S., CD8(+) T Cells Involved in Metabolic Inflammation in Visceral Adipose Tissue and Liver of Transgenic Pigs. *Front Immunol* **2021,** 12, 690069.
42. Miller, A. M., Role of IL-33 in inflammation and disease. *J Inflamm (Lond)* **2011,** 8, (1), 22.
43. Panganiban, R. P.; Vonakis, B. M.; Ishmael, F. T.; Stellato, C., Coordinated post-transcriptional regulation of the chemokine system: messages from CCL2. *J. Interferon Cytokine Res.* **2014,** 34, (4), 255-66.
44. Zielinska, K. A.; Van Moortel, L.; Opdenakker, G.; De Bosscher, K.; Van den Steen, P. E., Endothelial Response to Glucocorticoids in Inflammatory Diseases. *Front Immunol* **2016,** 7, 592.

45. Gruver-Yates, A. L.; Cidlowski, J. A., Tissue-specific actions of glucocorticoids on apoptosis: a double-edged sword. *Cells* **2013,** 2, (2), 202-23.
46. Shah, O. J.; Iniguez-Lluhi, J. A.; Romanelli, A.; Kimball, S. R.; Jefferson, L. S., The activated glucocorticoid receptor modulates presumptive autoregulation of ribosomal protein S6 protein kinase, p70 S6K. *J. Biol. Chem.* **2002,** 277, (4), 2525-33.
47. Shah, O. J.; Kimball, S. R.; Jefferson, L. S., Acute attenuation of translation initiation and protein synthesis by glucocorticoids in skeletal muscle. *Am J Physiol Endocrinol Metab* **2000,** 278, (1), E76-82.
48. Meyuhas, O.; Baldin, V.; Bouche, G.; Amalric, F., Glucocorticoids repress ribosome biosynthesis in lymphosarcoma cells by affecting gene expression at the level of transcription, posttranscription and translation. *Biochim. Biophys. Acta* **1990,** 1049, (1), 38-44.
49. Munzel, T.; Templin, C.; Cammann, V. L.; Hahad, O., Takotsubo Syndrome: Impact of endothelial dysfunction and oxidative stress. *Free Radic. Biol. Med.* **2021,** 169, 216-223.
50. Fabi, M.; Petrovic, B.; Andreozzi, L.; Corinaldesi, E.; Filice, E.; Biagi, C.; Rizzello, A.; Mattesini, B. E.; Bugani, S.; Lanari, M., Circulating Endothelial Cells: A New Possible Marker of Endothelial Damage in Kawasaki Disease, Multisystem Inflammatory Syndrome in Children and Acute SARS-CoV-2 Infection. *Int J Mol Sci* **2022,** 23, (17).
51. Tao, R.; Wang, Z. F.; Qiu, W.; He, Y. F.; Yan, W. Q.; Sun, W. Y.; Li, H. J., Role of S100A3 in human hepatocellular carcinoma and the anticancer effect of sodium cantharidinate. *Exp Ther Med* **2017,** 13, (6), 2812-2818.
52. Rogers, P. R.; Song, J.; Gramaglia, I.; Killeen, N.; Croft, M., OX40 promotes Bcl-xL and Bcl-2 expression and is essential for long-term survival of CD4 T cells. *Immunity* **2001,** 15, (3), 445-55.
53. Frazzi, R., BIRC3 and BIRC5: multi-faceted inhibitors in cancer. *Cell Biosci* **2021,** 11, (1), 8.
54. Hoh, J. F.; Hughes, S., Myogenic and neurogenic regulation of myosin gene expression in cat jaw-closing muscles regenerating in fast and slow limb muscle beds. *J. Muscle Res. Cell Motil.* **1988,** 9, (1), 59-72.
55. Hu, Y. W.; Wu, S. G.; Zhao, J. J.; Ma, X.; Lu, J. B.; Xiu, J. C.; Zhang, Y.; Huang, C.; Qiu, Y. R.; Sha, Y. H.; Gao, J. J.; Wang, Y. C.; Li, S. F.; Zhao, J. Y.; Zheng, L.; Wang, Q., VNN1 promotes atherosclerosis progression in apoE-/- mice fed a high-fat/high-cholesterol diet. *J. Lipid Res.* **2016,** 57, (8), 1398-411.
56. Huang, S. Y.; Liu, Y. H.; Chen, Y. J.; Yeh, Y. Y.; Huang, H. M., CD69 partially inhibits apoptosis and erythroid differentiation via CD24, and their knockdown increase imatinib sensitivity in BCR-ABL-positive cells. *J. Cell. Physiol.* **2018,** 233, (9), 7467-7479.
57. Barcellos-de-Souza, P.; Canetti, C.; Barja-Fidalgo, C.; Arruda, M. A., Leukotriene B(4) inhibits neutrophil apoptosis via NADPH oxidase activity: redox control of NF-kappaB pathway and mitochondrial stability. *Biochim. Biophys. Acta* **2012,** 1823, (10), 1990-7.
58. Wang, C. Y.; Mayo, M. W.; Korneluk, R. G.; Goeddel, D. V.; Baldwin, A. S., Jr., NF-kappaB antiapoptosis: induction of TRAF1 and TRAF2 and c-IAP1 and c-IAP2 to suppress caspase-8 activation. *Science* **1998,** 281, (5383), 1680-3.
59. Shiozaki, A.; Marunaka, Y.; Otsuji, E., Roles of Ion and Water Channels in the Cell Death and Survival of Upper Gastrointestinal Tract Cancers. *Front Cell Dev Biol* **2021,** 9, 616933.
60. Duan, C.; Allard, J. B., Insulin-Like Growth Factor Binding Protein-5 in Physiology and Disease. *Front Endocrinol (Lausanne)* **2020,** 11, 100.
61. Islam, M. A.; Sooro, M. A.; Zhang, P., Autophagic Regulation of p62 is Critical for Cancer Therapy. *Int J Mol Sci* **2018,** 19, (5).
62. Gugnoni, M.; Sancisi, V.; Manzotti, G.; Gandolfi, G.; Ciarrocchi, A., Autophagy and epithelial-mesenchymal transition: an intricate interplay in cancer. *Cell Death Dis* **2016,** 7, (12), e2520.
63. Orenstein, J. M.; Shulman, S. T.; Fox, L. M.; Baker, S. C.; Takahashi, M.; Bhatti, T. R.; Russo, P. A.; Mierau, G. W.; de Chadarevian, J. P.; Perlman, E. J.; Trevenen, C.; Rotta, A. T.; Kalelkar, M. B.; Rowley, A. H., Three linked vasculopathic processes characterize kawasaki disease: a light and transmission electron microscopic study. *PloS one* **2012,** 7, (6), e38998.
64. Shimizu, C.; Oharaseki, T.; Takahashi, K.; Kottek, A.; Franco, A.; Burns, J. C., The role of TGF-beta and myofibroblasts in the arteritis of Kawasaki disease. *Hum. Pathol.* **2013,** 44, (2), 189-98.
65. Bolli, R.; Marban, E., Molecular and cellular mechanisms of myocardial stunning. *Physiol. Rev.* **1999,** 79, (2), 609-34.
66. Myers, V. D.; McClung, J. M.; Wang, J.; Tahrir, F. G.; Gupta, M. K.; Gordon, J.; Kontos, C. H.; Khalili, K.; Cheung, J. Y.; Feldman, A. M., The Multifunctional Protein BAG3: A Novel Therapeutic Target in Cardiovascular Disease. *JACC Basic Transl Sci* **2018,** 3, (1), 122-131.
67. Shokr, M.; Rashed, A.; Lata, K.; Kondur, A., Dexamethasone Associated ST Elevation Myocardial Infarction Four Days after an Unremarkable Coronary Angiogram-Another Reason for Cautious Use of Steroids: A Case Report and Review of the Literature. *Case Rep Cardiol* **2016,** 2016, 4970858.
68. Rogers, K. M.; Bonar, C. A.; Estrella, J. L.; Yang, S., Inhibitory effect of glucocorticoid on coronary artery endothelial function. *Am J Physiol Heart Circ Physiol* **2002,** 283, (5), H1922-8.
69. Jun, S. S.; Chen, Z.; Pace, M. C.; Shaul, P. W., Glucocorticoids downregulate cyclooxygenase-1 gene expression and prostacyclin synthesis in fetal pulmonary artery endothelium. *Circ. Res.* **1999,** 84, (2), 193-200.
70. Feldstein, L. R.; Tenforde, M. W.; Friedman, K. G.; Newhams, M.; Rose, E. B.; Dapul, H.; Soma, V. L.; Maddux, A. B.; Mourani, P. M.; Bowens, C.; Maamari, M.; Hall, M. W.; Riggs, B. J.; Giuliano, J. S., Jr.; Singh, A. R.; Li, S.; Kong, M.; Schuster, J. E.; McLaughlin, G. E.; Schwartz, S. P.; Walker, T. C.; Loftis, L. L.; Hobbs, C. V.; Halasa, N. B.; Doymaz, S.; Babbitt, C. J.; Hume, J. R.; Gertz, S. J.; Irby, K.; Clouser, K. N.; Cvijanovich, N. Z.; Bradford, T. T.; Smith, L. S.; Heidemann, S. M.; Zackai, S. P.; Wellnitz, K.; Nofziger, R. A.; Horwitz, S. M.; Carroll, R. W.; Rowan, C. M.; Tarquinio, K. M.; Mack, E. H.; Fitzgerald, J. C.; Coates, B. M.; Jackson, A. M.; Young, C. C.; Son, M. B. F.; Patel, M. M.; Newburger, J. W.; Randolph, A. G.; Overcoming, C.-I., Characteristics and

Outcomes of US Children and Adolescents With Multisystem Inflammatory Syndrome in Children (MIS-C) Compared With Severe Acute COVID-19. *JAMA* **2021,** 325, (11), 1074-1087.

71. Valverde, I.; Singh, Y.; Sanchez-de-Toledo, J.; Theocharis, P.; Chikermane, A.; Di Filippo, S.; Kucinska, B.; Mannarino, S.; Tamariz-Martel, A.; Gutierrez-Larraya, F.; Soda, G.; Vandekerckhove, K.; Gonzalez-Barlatay, F.; McMahon, C. J.; Marcora, S.; Napoleone, C. P.; Duong, P.; Tuo, G.; Deri, A.; Nepali, G.; Ilina, M.; Ciliberti, P.; Miller, O.; Team*, A. C.-R. R., Acute Cardiovascular Manifestations in 286 Children With Multisystem Inflammatory Syndrome Associated With COVID-19 Infection in Europe. *Circulation* **2021,** 143, (1), 21-32.
72. Bermejo, I. A.; Bautista-Rodriguez, C.; Fraisse, A.; Voges, I.; Gatehouse, P.; Kang, H.; Piccinelli, E.; Rowlinson, G.; Lane, M.; Semple, T.; Moscatelli, S.; Dwornik, M.; Lota, A.; Di Salvo, G.; Wage, R.; Prasad, S. K.; Mohiaddin, R.; Pennell, D. J.; Thavendiranathan, P.; Krupickova, S., Short-Term sequelae of Multisystem Inflammatory Syndrome in Children Assessed by CMR. *JACC Cardiovasc Imaging* **2021,** 14, (8), 1666-1667.
73. Penner, J.; Abdel-Mannan, O.; Grant, K.; Maillard, S.; Kucera, F.; Hassell, J.; Eyre, M.; Berger, Z.; Hacohen, Y.; Moshal, K.; Group, G. P.-T. M., 6-month multidisciplinary follow-up and outcomes of patients with paediatric inflammatory multisystem syndrome (PIMS-TS) at a UK tertiary paediatric hospital: a retrospective cohort study. *Lancet Child Adolesc Health* **2021,** 5, (7), 473-482.
74. Ciftel, M.; Ates, N.; Yilmaz, O., Investigation of endothelial dysfunction and arterial stiffness in multisystem inflammatory syndrome in children. *Eur. J. Pediatr.* **2022,** 181, (1), 91-97.
75. Anderson, P., Post-transcriptional regulons coordinate the initiation and resolution of inflammation. *Nat Rev Immunol* **2010,** 10, (1), 24-35.
76. Holz, M. K.; Ballif, B. A.; Gygi, S. P.; Blenis, J., mTOR and S6K1 mediate assembly of the translation preinitiation complex through dynamic protein interchange and ordered phosphorylation events. *Cell* **2005,** 123, (4), 569-80.
77. Maurya, M. R.; Gupta, S.; Li, J. Y.; Ajami, N. E.; Chen, Z. B.; Shyy, J. Y.; Chien, S.; Subramaniam, S., Longitudinal shear stress response in human endothelial cells to atheroprone and atheroprotective conditions. *Proc. Natl. Acad. Sci. U. S. A.* **2021,** 118, (4).
78. McCrindle, B. W.; Rowley, A. H.; Newburger, J. W.; Burns, J. C.; Bolger, A. F.; Gewitz, M.; Baker, A. L.; Jackson, M. A.; Takahashi, M.; Shah, P. B.; Kobayashi, T.; Wu, M. H.; Saji, T. T.; Pahl, E.; American Heart Association Rheumatic Fever, E.; Kawasaki Disease Committee of the Council on Cardiovascular Disease in the, Y.; Council on, C.; Stroke, N.; Council on Cardiovascular, S.; Anesthesia; Council on, E.; Prevention, Diagnosis, Treatment, and Long-Term Management of Kawasaki Disease: A Scientific Statement for Health Professionals From the American Heart Association. *Circulation* **2017,** 135, (17), e927-e999.
79. Prevention., C. f. D. C. a., Multisystem Inflammatory Syndrome in Children (MIS-C) Associated with Coronavirus Disease 2019 (COVID-19). *Emergency Preparedness and Response.* **2021,** Published November 1, 2021., https://emergency.cdc.gov/han/2020/han00432.asp
80. Chen, S.; Zhou, Y.; Chen, Y.; Gu, J., fastp: an ultra-fast all-in-one FASTQ preprocessor. *Bioinformatics* **2018,** 34, (17), i884-i890.
81. Ewels, P.; Magnusson, M.; Lundin, S.; Kaller, M., MultiQC: summarize analysis results for multiple tools and samples in a single report. *Bioinformatics* **2016,** 32, (19), 3047-8.
82. Patro, R.; Duggal, G.; Love, M. I.; Irizarry, R. A.; Kingsford, C., Salmon provides fast and bias-aware quantification of transcript expression. *Nat Methods* **2017,** 14, (4), 417-419.
83. Love, M. I.; Huber, W.; Anders, S., Moderated estimation of fold change and dispersion for RNA-seq data with DESeq2. *Genome Biol* **2014,** 15, (12), 550.
84. Langfelder, P.; Horvath, S., WGCNA: an R package for weighted correlation network analysis. *BMC Bioinformatics* **2008,** 9, 559.